

Inelastic Light Scattering Studies of $\text{Bi}_2\text{Sr}_2\text{CaCu}_2\text{O}_{8+\delta}$: Charge and Spin Excitations Revisited

Hsiang-Lin Liu*

Department of Physics, National Taiwan Normal University, Taipei 116, Taiwan

We revisit the low- and high-energy Raman scattering spectra of $\text{Bi}_2\text{Sr}_2\text{CaCu}_2\text{O}_{8+\delta}$ single crystals. We show that the superconductivity phase transition results not only in a renormalization of the in-plane and out-of-plane electronic scattering continuum, but also in an enhancement of the intensity of the two-magnon excitation. These results suggest that the subtle interplay between the electronic and magnetic degrees of freedom must be taken into account in a proper description of cuprate superconductors.

PACS numbers: 74.25.Gz, 74.72.Hs

I. INTRODUCTION

Inelastic light scattering spectroscopy has emerged as one of the effective tools for studying the doping-temperature phase diagram of the high- T_c cuprates, in which the magnetically ordered, metallic, and superconducting phases exist in close proximity. This technique affords a means by which energy and symmetry information regarding electronic and spin excitations can be simultaneously explored, and indeed provides special insight into the nature of cuprate high temperature superconductivity.

Going from well-defined magnons (in the Néel undoped state) related to the localized copper spins to a Fermi liquid picture (at the highest doping available), Raman scattering experiments cover a whole range of situations where the charge and spin responses are intimately linked and reveal a number of key features: First, two-magnon Raman scattering from the insulating parent compounds of high- T_c superconductors contains information not only on the magnetic interaction in the CuO_2 planes, but also on the electronic properties in these materials [1]. Importantly, the two-magnon peak position yields the first estimate of Cu-O-Cu nearest neighbor superexchange interaction constant, J , in La_2CuO_4 [2]. Second, with doping the carriers the cuprate materials become metallic and no longer have a long-range antiferromagnetic order. The two-magnon Raman scattering directly probes magnetic fluctuations in a state of short-range antiferromagnetic order [3–5]. In addition, for these doped high- T_c superconductors, the Raman spectra exhibit a strongly polarization-dependent electronic continuum over a broad range of frequencies [6]. The continuum intensity provides information on the incoherent scattering of the quasiparticles on different regions of the Fermi surface [7]. Below T_c , the continuum redistributes; the intensity at low energies is decreasing and the increasing intensity at high energies gives the 2Δ peak-like feature. The doping and symmetry dependences of the 2Δ peak offer

an alternative to tunneling and angle-resolved photoemission spectroscopies (ARPES) as a probe of the superconducting energy gap [8].

In this paper, we revisit the results of a polarized Raman scattering investigation of high quality $\text{Bi}_2\text{Sr}_2\text{CaCu}_2\text{O}_{8+\delta}$ (Bi-2212) single crystals aimed at simultaneously exploring the evolution of charge and spin response associated with the superconducting transition. We show that there is a superconductivity-induced effect on the low- and high-energy electronic scattering continuum as well as the two-magnon excitation. More interestingly, below T_c , the c -axis electronic continuum redistributes for energies extending to 40Δ .

II. EXPERIMENTAL

Single crystals of Bi-2212 were grown near-stoichiometric using a solvent-free floating zone process in a double-mirror image furnace modified for very slow growth. We have repeatedly studied the same single crystal of dimensions $5 \times 1 \times 0.5 \text{ mm}^3$ with annealing under various conditions. The superconducting transition determined by a dc magnetization measurement gave overdoped (onset $T_c = 84 \text{ K}$, $\Delta T_c = 4 \text{ K}$), slightly overdoped ($T_c = 92 \text{ K}$, $\Delta T_c = 2 \text{ K}$), optimally doped ($T_c = 95 \text{ K}$, $\Delta T_c = 1 \text{ K}$), and underdoped ($T_c = 87 \text{ K}$, $\Delta T_c = 4 \text{ K}$). As an example, we show the detailed results of the slightly overdoped Bi-2212 sample. The polarized Raman measurements were performed on the ab plane of the sample surface as well as for photons polarized along the c -axis. The Raman spectra were taken in pseudobackscattering geometry with 406.7 and 647.1 nm photons from a Kr^+ laser. The laser excitation of less than 5 W/cm^2 was focused into a $50 \mu\text{m}$ diameter spot on the sample surface. The temperatures referred to in this paper are the nominal temperatures inside the cryostat. The spectra were analyzed by a triple grating spectrometer with a liquid-nitrogen cooled charge-coupled device detector. All the Raman spectra were corrected for the spectral response of the spectrometer and detector, the optical absorption of the sample as well as the refraction at the sample-gas interface [6]. Throughout this study, x and y are indexed along the Bi-O bonds, rotated by 45° with respect to the Cu-O bonds. All symmetries refer to a tetragonal D_{4h} point group.

III. RESULTS AND DISCUSSION

Fig. 1 shows the imaginary part of the Raman response function, $\text{Im}\chi(\omega)$, for the slightly overdoped sample ($T_c = 92 \text{ K}$) in the B_{1g} , B_{2g} , A_{1g} , and zz -polarized A_{1g} scattering geometries at two different temperatures, 100 K ($T > T_c$) and 5 K ($T \ll T_c$). $\text{Im}\chi(\omega)$ was obtained by dividing the measured spectra by the Bose-Einstein thermal factor. For the incident photon energy with 406.7 nm, we follow the spectra to 1 eV Raman shift. There are three notable features seen in the normal-state Raman scattering spectra: first, there are phonon peaks below 1500 cm^{-1} in both in-plane and out-of-plane A_{1g} spectra; second, all four scattering geometries show electronic continuum scattering intensity, the strength of which depends strongly on the polarization configuration; and third, the B_{1g} spectrum

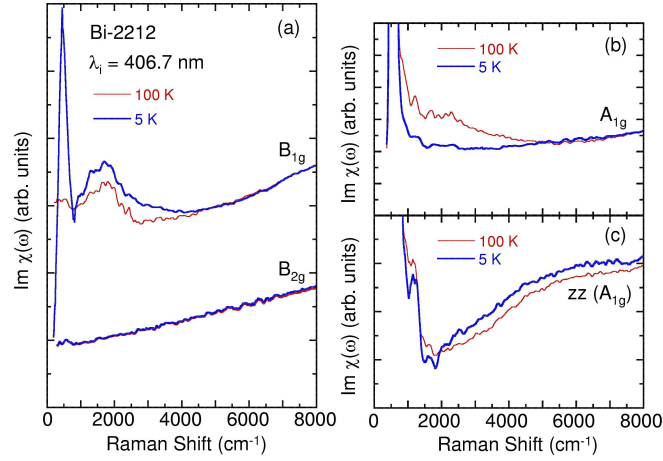


FIG. 1: The high-energy portion of the Raman scattering spectra taken in four different polarizations and using 406.7 nm excitation for the slightly overdoped sample ($T_c = 92$ K). The thick line denotes the spectra taken at 5 K and the thin line at 100 K.

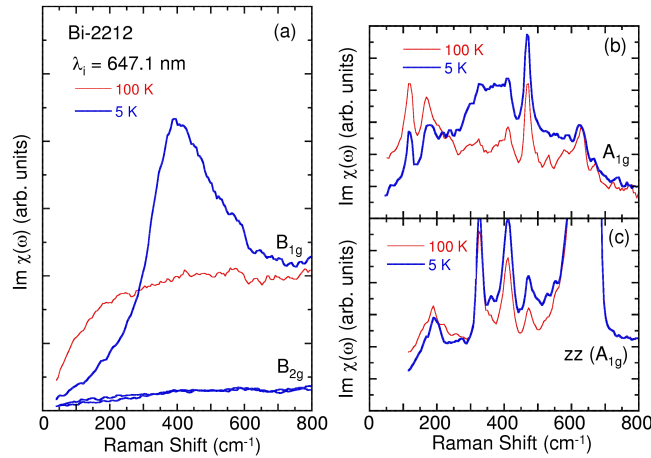


FIG. 2: The low-energy portion of the Raman scattering spectra taken in four different polarizations and using 647.1 nm excitation for the slightly overdoped sample ($T_c = 92$ K). The thick line denotes the spectra taken at 5 K and the thin line at 100 K.

exhibits a broad peak at around 1850 cm^{-1} , associated with the two-magnon excitation. In this paper, we are primarily interested in the superconductivity effects on the electronic and magnetic Raman scattering response.

Well below T_c , it can be seen in Fig. 1(a) that for the B_{1g} symmetry there is an intensity enhancement of the two-magnon peak and additional structure (so-called “ 2Δ

peak”) appears in the low-frequency spectrum, which peaks at around 440 cm^{-1} . While the B_{2g} spectra, above and below T_c , are essentially identical. In the superconducting state, the in-plane A_{1g} electronic Raman scattering intensity (Fig. 1(b)) exhibits a suppression between 1200 and 5000 cm^{-1} . More interestingly, for $T \ll T_c$ the rearrangement of the c -axis electronic Raman response (Fig. 1(c)) occurs over an energy range up to 8000 cm^{-1} . To demonstrate more clearly the effect of superconductivity on the low-frequency part of the electronic continuum, we show in Fig. 2 the Raman spectra for $\omega < 800 \text{ cm}^{-1}$. One first observes that the B_{1g} contribution (Fig. 2(a)) gives an electronic continuum that is much stronger than that in any other polarization. Below T_c , the strong suppression of the continuum is observed, and the low-frequency intensity varies roughly as ω^3 , while it is quite linear in the B_{2g} spectrum. Such ω dependences in both B_{1g} and B_{2g} continua are consistent with an order parameter of d -wave symmetry [$d_{(x^2-y^2)}$ when referred to Cu-O bonds] [8]. The superconducting transition also leads to the redistribution of the continuum into a broad peak around 370 cm^{-1} for the in-plane A_{1g} polarization (Fig. 2(b)), but the magnitude of superconductivity-induced peak is much less intense in A_{1g} symmetry than that found in B_{1g} symmetry. Notably, there is a decrease in the scattering strength of the c -axis continuum at low energies which redistributes into the weak and broad peak at higher frequencies (Fig. 2(c)), similar to the data observed in the ab -plane.

There are two main features of interest in Figs. 1 and 2. The first is the noticeable changes below T_c occurring in the electronic and magnetic contributions to the B_{1g} Raman scattering response. It has been shown that, based on the symmetry consideration [8], the B_{1g} Raman form factor probes the Fermi surface near the $[0, \pm \frac{\pi}{a}]$ and $[\pm \frac{\pi}{a}, 0]$ directions of the electronic Brillouin zone, where the two-magnon density of state is peaked near the antiferromagnetic Brillouin zone boundary. Therefore, the formation of 2Δ peak with a suppression of the scattering intensity at frequencies below the peak position and a concomitant increase in the intensity of the two-magnon peak at $T < T_c$ indicate that the electronic and magnetic scattering channels are both influenced by the superconducting transition. While the redistribution of the low-frequency spectral weight in the B_{1g} symmetry reflects a reduced or vanishing density of electronic states at the Fermi surface in the vicinity of the principal k_x and k_y axes when a superconducting gap opens. Simultaneously, the increasing scattering intensity of the two-magnon peak indicates an enhanced magnetic coherence in the superconducting state. This interplay between the low-frequency 2Δ and high-frequency two-magnon feature was also observed in the optimally doped and underdoped cuprates [5], signifying that there is a common physical mechanism underlying the apparently different phenomena that are observed in the charge and spin excitation channels.

The nature of the coupling between charge and spin degrees of freedom in the Raman scattering spectra can be more carefully explored by comparing the energy positions of the B_{1g} 2Δ and two-magnon peaks as function of hole doping p [9], as shown in Fig. 3. For a comparison, the newly observed results of the out-of-plane A_{1g} 2Δ peak and twice the value of the maximum superconducting gap obtained from the tunneling spectroscopy [10] as well as ARPES measurements [11] of the $(\pi, 0)$ gap (the d -wave maximum) for the same batch of Bi-2212 crystals are also included in Fig. 3. With decreasing doping, the B_{1g} 2Δ peak shifts

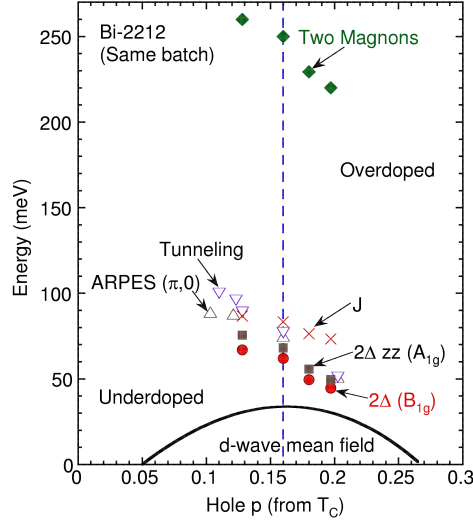


FIG. 3: Plot of the 2Δ peak position (taken at 5 K) and the two-magnon energy versus the hole concentration. For comparison, twice the value of Δ obtained from other experiments have also been plotted. Ref. [10] (down triangles) from tunneling and Ref. [11] (up triangles) from ARPES.

monotonically upward in energy despite a decrease in T_c . $2\Delta/k_B T_c$ changes from a value ~ 6 for overdoped Bi-2212 with $T_c = 84$ K to value approaching ~ 9 in the underdoped region. A similar trend was also observed for the ab -plane A_{1g} symmetry [12], but with smaller values of $2\Delta/k_B T_c$. Notably, the c -axis 2Δ peak, which has A_{1g} symmetry, is found at a higher frequency than that seen in the planar symmetries, but still less than twice the value of Δ from single electron spectroscopies [13], *i.e.*, $2\Delta(B_{1g}) < 2\Delta(zz) < 2\Delta$. We believe that the zz geometry produces a pair of quasiparticles in different CuO_2 planes, whereas the in-plane geometries produce the pair on the same CuO_2 plane. These Raman results tell us that, starting with the superconducting condensate, it costs more energy to create a quasiparticle pair in different planes than in the same plane. The two kinds of pairs could be expected to undergo different final state interactions and screening corrections. Such final state interactions renormalize the magnitude of the superconducting gap. In addition to the 2Δ feature, the two-magnon peak position shifts with decreasing doping towards increasing energies. The analogy in doping dependence of the superexchange interaction constant, J , and the superconducting gap, 2Δ , suggests that the antiferromagnetic magnons might play a more important role in high- T_c cuprates than has been suspected.

IV. SUMMARY

In summary, we have investigated the polarized Raman spectra of charge and spin excitations in Bi-2212 single crystals with various oxygen concentrations. Our study provides clear evidence of the superconductivity-induced renormalization of the low- and high-energy electronic scattering continuum, and a concomitant enhancement of the intensity of the two-magnon peak. These results suggest that the nature of the interaction between the electronic and magnetic degrees of freedom is crucial for understanding of the observed unconventional non-BCS behavior of the cuprates. Moreover, new evidence for the superconductivity-induced effect on the c -axis electronic continuum extending to the frequencies as high as 40Δ is observed, signifying the distinctly different dynamics of quasi-particles created with out-of-plane polarization.

Acknowledgments

Much of the work described here was done in collaboration with M. V. Klein, G. Blumberg, M. Rübhausen, P. Guptasarma, and D. G. Hinks. This work was supported by the National Science Council of Republic of China under Grant No. NSC 93-2112-M-003-005 and the National Taiwan Normal University under Grant No. ORD93-B.

References

- * Electronic address: hliu@phy.ntnu.edu.tw
- [1] Andrey V. Chubukov and David M. Frenkel, Phys. Rev. B **52**, 9760 (1995); Dirk K. Morr and Andrey V. Chubukov, *ibid.*, **56**, 9134 (1997).
 - [2] K. B. Lyons *et al.*, Phys. Rev. Lett. **60**, 732 (1988); Phys. Rev. B **37**, 2353 (1988); S. Sugai *et al.*, Phys. Rev. B **38**, 6436 (1988); P. E. Sulewsky *et al.*, Phys. Rev. B **41**, 225 (1990).
 - [3] G. Blumberg *et al.*, Phys. Rev. B **49**, 13295 (1994); G. Blumberg *et al.*, *ibid.* **53**, R11930 (1996).
 - [4] G. Blumberg *et al.*, Science **276**, 1427 (1997).
 - [5] M. Rübhausen *et al.*, Phys. Rev. B **56**, 14797 (1997); *ibid.*, **58**, 3462 (1998).
 - [6] D. Reznik *et al.*, Phys. Rev. B **46**, 11725 (1992); D. Reznik *et al.*, *ibid.* **48**, 7624 (1993).
 - [7] C. M. Varma *et al.*, Phys. Rev. Lett. **63**, 1996 (1989); B. S. Shastry and B. I. Shraiman, *ibid.* **65**, 1068 (1990); B. S. Shastry and B. I. Shraiman, Int. J. Mod. Phys. B **5**, 365 (1991); A. Virosztek and J. Ruvalds, Phys. Rev. B **45**, 347 (1992).
 - [8] T. P. Devereaux and A. P. Kampf, Int. J. Mod. Phys. B **11**, 2093 (1997).
 - [9] Each T_c is converted to p using the empirical relation $T_c/T_{c,\max} = 1 - 82.6(p - 0.16)^2$.
 - [10] Y. DeWilde *et al.*, Phys. Rev. Lett. **80**, 153 (1998); N. Miyakawa *et al.*, *ibid.* **80**, 157 (1998).
 - [11] M. R. Norman *et al.*, Nature (London) **392**, 157 (1998).
 - [12] C. Kendziora and A. Rosenberg, Phys. Rev. B **52**, R9867 (1995).
 - [13] H. L. Liu *et al.*, Phys. Rev. Lett. **82**, 3524 (1999).